Title Page

Mechanisms and seasonal drivers of calcification in the temperate coral *Turbinaria reniformis* at its latitudinal limits

Authors:

Claire L Ross[1,2], Verena Schoepf[1,2], Thomas M DeCarlo[1,2], Malcolm T McCulloch[1,2]

Affiliations:

[1]Oceans Institute and School of Earth Sciences, The University of Western Australia, 35 Stirling Hwy, Crawley WA 6009, Australia

[2]ARC Centre of Excellence for Coral Reef Studies, The University of Western Australia, 35 Stirling Hwy, Crawley WA 6009, Australia

Abstract

High-latitude coral reefs provide natural laboratories for investigating the mechanisms and limits of coral calcification. While the calcification processes of tropical corals have been studied intensively, little is known about how their temperate counterparts grow under much lower temperature and light conditions. Here we report the results of a long-term (2-year) study of seasonal changes in calcification rates, photo-physiology, and calcifying fluid (cf) chemistry (using boron isotope systematics and Raman spectroscopy) for the coral *Turbinaria reniformis* growing near its latitudinal limits (34.5°S) along the southern coast of Western Australia. In contrast to tropical corals, calcification rates were found to be three-fold higher during winter (16 to 17°C) compared to summer (~21°C), and negatively correlated with light, but had no correlation with temperature. These unexpected findings are attributed to a combination of higher chlorophyll *a* and hence increased heterotrophy during winter compared to summer together with the corals' ability to seasonally modulate pH_{cf}, with carbonate ion concentration $[CO_3^{2-}]_{cf}$ being the main controller of calcification rates. Conversely, calcium ion concentration $[Ca^{2+}]_{cf}$ declined with increasing calcification rates; resulting in aragonite saturation states Ω_{cf} that were stable yet elevated by x4 above seawater values. Our results show that corals growing near their latitudinal limits exert strong physiological control over their calcifying fluid in order to maintain year-round calcification rates that are insensitive to the unfavourable temperature regimes typical of high-latitude reefs.

Introduction

Symbiotic corals are the foundation species of coral reef ecosystems, creating complex 3-dimensional habitats that harbour over one third of the oceans' biodiversity [1]. Their distribution spans almost 70 degrees of latitude, occupying a range of environments from tropical equatorial regions to cold temperate zones [2]. However, the future of these highly diverse and widespread ecosystems is threatened by the unprecedented impacts of both CO_2-driven ocean acidification (OA) and warming [3]. Abrupt El Niño-Southern Oscillation (ENSO) driven ocean warming events cause widespread coral bleaching and mortality due to the loss of the algal symbiont [4,5], while declines in seawater pH and carbonate ion concentrations ($[CO_3^{2-}]$) due to OA have often been shown to cause declines in coral calcification rates (e.g.[6,7]).

However, the effects of OA and rising seawater temperatures on symbiotic corals are likely to vary geographically. For example, high-latitude reefs (i.e. above 28°N and below 28°S) are already considered marginal, in part due to their low seawater aragonite saturation state (Ω), and will experience further declines in Ω due to OA, making them less suitable to support coral calcification [3]. In contrast, warming seawater temperatures may have a positive net effect on high-latitude coral calcification rates, particularly during winter when lower temperatures currently limit calcification rates [8–11]. However, during winter increased heterotrophic feeding at high-latitude may help to offset the negative influences of lower temperatures and Ω_{sw} by providing corals with the energy required for calcification processes [12,13]. Furthermore, while high-latitude warming would be expected to enhance coral calcification rates, and hence outweigh the negative effects of OA, increases to summer-time temperatures beyond localised thermal optimums may cause bleaching and declines to calcification [5,14]. Given the wide range of possible responses, and that atmospheric CO_2 concentrations are projected to continue increasing even under stringent emissions reduction scenarios, it is therefore critical to better understand the coral calcification mechanisms and strategies available for corals at high-latitude to endure ocean warming and acidification [15,16].

One such strategy to cope with and acquire resistance to OA is the corals' ability to modulate chemical conditions at the site of calcification (e.g.[15–20]). Reef-building corals create their calcium carbonate ($CaCO_3$) skeletons within a seawater supplied, semi-isolated extracellular calcifying fluid (cf), located between the sub-calicoblastic cells and the skeleton [21]. While this process is highly biologically modulated [21], the reaction kinetics are still

nevertheless dependent on temperature and Ω in the calcifying fluid [22]. Although aragonite is already supersaturated in ambient seawater (i.e. $\Omega > 3$), corals possess mechanisms to up-regulate both pH_{cf} and dissolved inorganic carbon (DIC_{cf}) to increase Ω_{cf} above seawater levels (i.e. ~10 to 25) [15,17,18], and thus promote rapid $CaCO_3$ growth [22]. Additionally, the counter-regulation of pH_{cf} and DIC_{cf} on seasonal timescales [18] may also act to dampen the effect of seasonally variable temperature on high-latitude calcification rates (see [23]). Thus, while laboratory experiments have demonstrated that declines in coral pH_{cf} still typically occur under OA (e.g.[17,24]), it is clear that the corals' strong ability to up-regulate pH_{cf} and DIC_{cf} is a critical mechanism for calcification, and provides corals with some resistance against the negative impacts of OA (e.g.[16,18]).

The ability to infer the calcium ion concentrations in the calcifying fluid ($[Ca^{2+}]_{cf}$), pH_{cf}, DIC_{cf} and Ω_{cf}, however, has only recently become feasible due to the development of new geochemical approaches using boron isotope ($\delta^{11}B$) and elemental (B/Ca) systematics [18], together with Raman spectroscopy [25,26]. Thus, until recently, typically one [17,20,24,27] or at most two (e.g.[18,28]) aspects of the calcifying fluid chemistry (i.e. pH and CO_3^{2-}) have been measured. Quantifying $[Ca^{2+}]_{cf}$ remains, to date, a key knowledge gap given that $[Ca^{2+}]_{cf}$ is a critical component of the coral calcification process. While it is often assumed that $[Ca^{2+}]_{cf}$ is equal or similar to seawater, direct measurements of $[Ca^{2+}]_{cf}$ are particularly limited. Recent work combining Raman spectroscopy with boron systematics suggests that active elevation of $[Ca^{2+}]$ in the calcifying fluid (up to 25% higher than seawater) may be fundamental to the resistance of calcification to OA for some species [26]. Prior to that, the only other $[Ca^{2+}]_{cf}$ measurements were made using micro-sensors, which showed that $[Ca^{2+}]_{cf}$ was elevated above seawater by ~10% [29]. Yet, $[Ca^{2+}]_{cf}$ concentrations may play an important role in controlling Ω_{cf} in addition to $[CO_3^{2-}]_{cf}$. Thus, all components of the calcifying fluid carbonate chemistry need to be quantified to understand the mechanisms and responses of coral calcification to changing environmental conditions.

Here, we combine novel geochemical analyses (Raman spectroscopy and boron systematics) to quantify calcifying fluid chemistry (i.e. pH_{cf}, DIC_{cf}, $CO_3^{2-}{}_{cf}$, $Ca^{2+}{}_{cf}$, and Ω_{cf}), together with calcification rates and photo-physiology as a proxy for coral health (photochemical efficiency; F_v/F_m) for the high-latitude coral species *Turbinaria reniformis* growing near the latitudinal limits for hermatypic coral growth in Bremer Bay, Western Australia (WA; 34.5°S; 17°C to 21°C). We show how corals seasonally regulate their calcifying fluid chemistry to optimise calcification rates at high-latitude. Our study is the first

to constrain both aspects of Ω_{cf} (i.e. CO_3^{2-} and Ca^{2+}) as well as pH_{cf} for corals growing in situ. Informed by this unique dataset, we present a conceptual model to elucidate the mechanisms of high-latitude coral calcification with respect to the full suite of carbonate system dynamics within the calcifying fluid.

Materials and Methods

Study sites and overview

Bremer Bay is located approximately 500 km south-east of Perth in WA, bordering the Southern Ocean (34.4°S, 119.4°E; Fig. 1a). These waters support 7 symbiotic species of coral, which likely migrated southwards via the Leeuwin Current; a pole-wards flowing current that transports warm water along the WA coastline [30]. *T. reniformis* is the dominant coral species at this location, with 100% coral cover in some areas, surrounded by macro-algae and seagrass. Seasonal mean monthly seawater temperatures typically range from just 17°C to 21°C, and light levels range from 13.5 to 21 mol m^{-2} d^{-1} (Fig. 1b-c).

We measured coral calcification rates, linear extension rates, photo-physiology (F_v/F_m), and analysed the chemical composition of the calcifying fluid for *T. reniformis* at two sites in Bremer Bay: Back Beach (herein entitled Site 1; ~9 m water depth) and Little Boat Harbour (herein entitled Site 2; ~7 m water depth) (Fig. 1a). Measurements were taken every 3 to 4 months over a ~2-year period between December 2014 and October 2016. See Electronic supplementary for additional details.

Environmental measurements and the 2016 El Niño

Photosynthetically active radiation (PAR), temperature, salinity, pH on the total scale (pH_T), Total Alkalinity (TA), and nutrients (ammonium, nitrate + nitrite, and phosphate) were measured throughout the study as per previously published methodology [31]. Monthly satellite-derived chlorophyll *a* for Bremer Bay was obtained from the Integrated Marine Observing System (IMOS [32]; Supplementary Fig. S1). The 2015/16 global El Niño caused anomalously cold-water conditions during the 2016 winter in southwest WA. Seasonal seawater temperatures in Bremer Bay during the 2016 El Niño winter were, on average, up to 1°C cooler than the 20-year long-term average (IMOS, 2017); highlighting the chronically cold winter events (16°C) that high-latitude corals must cope with. Further details are provided in the electronic supplementary material.

Photo-physiology

The maximal quantum yield of electron transport through photosystem II (F_v/F_m) was measured using a Diving-PAM (Walz, Germany). Measurements of F_v/F_m were performed after one hour of dark acclimation. The fibre optic probe on the PAM fluorometer was kept at a fixed distance (5 mm) using plastic tubing. The PAM settings used were: measuring intensity (3), gain (3), saturation intensity (12), and signal width (0.8).

Coral calcification and linear extension rates

Calcification rates (mg $CaCO_3$ cm^{-2} d^{-1}) were measured on 35 individual coral colonies (n = 21 at Site 1 and n = 14 at Site 2) using samples taken from the natural population (1 sample per parent colony, located ~3 to 5 m apart). The sample specimens were mounted on plastic tiles, and deployed in situ on aluminium frames (see [31]). Changes in weight were measured using the buoyant weight technique [33], and then normalised to surface area using a regression between surface area (measured using Image J Software [14]) and dry weight (9 to 190 g; n = 23, r^2 = 0.98; Supplementary Fig. S2). Linear extension rates were measured on naturally growing coral colonies at Site 2 only. We marked these corals with semi-permanent reference points by drilling 3 separate nails into 2 colonies. The extension rates were measured by taking the distance (± 1mm) from the reference point to the growing edge at three-month intervals. Geochemical studies (see following) were undertaken on the outmost growing tips of specimens sampled every three months over the ~ 2 year period.

Geochemical analyses

We used Raman spectroscopy to determine Ω_{cf}, and boron systematics ($\delta^{11}B$, B/Ca) to determine coral pH_{cf}, $[CO_3^{2-}]_{cf}$, and by inference $[Ca^{2+}]_{cf}$. Previous protocols were used for analysis of trace elements and boron isotopes (see [18,23]) and Raman spectroscopy [25]. Sampling distances of the coral skeletons were based on linear extension measurements (0.3 to 1.5 mm month ^{1}; Supplementary Table 1). Additionally we used the molar ratios of strontium to calcium (Sr/Ca) and lithium to magnesium (Li/Mg) temperature proxies to confirm the seasonal chronology of skeletal growth histories.

The pH_{cf} was derived from the measured skeletal $\delta^{11}B$ values according to the following equation [34]:

$$pH_{cf} = \frac{pK_B - Log\{[\delta^{11}B_{sw} - \delta^{11}B_{carb}]}{[\alpha_B \delta^{11}B_{carb} - \delta^{11}B_{sw} + 1000(1.0272-1]\}} \quad (1)$$

where pK_B is the dissociation constant of boric acid in seawater [35] at the temperature and salinity of the seawater in Bremer Bay, $\delta^{11}B_{carb}$ and $\delta^{11}B_{SW}$ are the boron

isotopic composition of the coral skeleton and average seawater (39.61‰), respectively, and α_B is the isotopic fractionation factor (1.0272) [36].

We estimated $[CO_3^{2-}]_{cf}$ using molar ratios of boron to calcium (B/Ca) according to the following relationship [18,37]:

$$[CO_3^{2-}]_{cf} = \frac{[B(OH)_4^-]_{cf} K_D^{B/Ca}}{[\frac{B}{Ca}]_{arag}} \quad (2)$$

where $[B(OH)_4^-]_{cf}$ is the concentration of borate in the calcifying fluid, $K_D^{B/Ca}$ is the distribution coefficient for boron between aragonite and seawater [18], and $[B/Ca]_{arag}$ is the elemental ratio of boron to calcium measured in the coral skeleton. The concentration of DIC_{cf} was then calculated from the estimates of pH_{cf} and $[CO_3^{2-}]_{cf}$ [18,28].

Raman spectroscopy was conducted to determine Ω_{cf} using an abiogenic calibration to peak width [25]. Finally, the $[Ca^{2+}]_{cf}$ was inferred from Ω_{cf} (Raman) and $[CO_3^{2-}]_{cf}$ ($\delta^{11}B$ and B/Ca) according to the following relationship:

$$[Ca^{2+}]_{cf} = \frac{\Omega_{cf} K_{sp}}{[CO_3^{2-}]_{cf}} \quad (3)$$

where K^*_{sp} is the solubility constant for aragonite as a function of temperature and salinity, Ω_{cf} is the saturation state of the calcifying fluid determined from Raman, and $[CO_3^{2-}]_{cf}$ is the carbonate ion concentration of the calcifying fluid estimated from $\delta^{11}B$ and B/Ca (Eq. 2). See electronic supplementary material for additional details.

Statistical analyses

A t-test was used to test for significant differences in calcification rates between the October 2015 time point and the October 2016 (unusually cold El Niño) time point. Repeated measures analysis of variance (rANOVA) was used to test for the effect of site on coral calcification rate, F_v/F_m, DIC_{cf}, pH_{cf}, $[CO_3^{2-}]_{cf}$, $[Ca^{2+}]_{cf}$, and Ω_{cf}. Linear regression analysis was used to examine relationships between coral calcification rate, F_v/F_m, calcifying fluid parameters, and environmental data. See electronic supplementary material for additional details.

Results

Environmental conditions

On average, monthly averaged seawater temperatures ranged from 16° to 21°C (Fig. 1b). Site 2 showed cold temperature 'spikes' during January and February 2016 that were not evident at Site 1 (Fig. 1b). However, for all months except January and February 2016, differences in mean temperatures generally did not differ by more than 0.30 °C. The light

attenuation coefficient (k_d) measured for seawater was very low, signifying high water clarity (~0.06 m^{-1} in summer and ~0.07 m^{-1} in winter; Supplementary Table 3). On average, monthly averaged seasonal PAR reaching the benthos ranged from 9.8 to 22.3 mol m^{-2} d^{-1} at Site 1 and 10.8 to 26 mol m^{-2} d^{-1} at Site 2 (Fig. 1c). Diurnal measurements of ambient seawater pH (Supplementary Fig. S3) showed that the pH of near shore waters in Bremer Bay varied minimally (0.06 pH units) between seasons (8.05 in summer to 8.11 in winter; Supplementary Table 3). Seawater Ω_{ar} was, on average, ~3.0 based on daytime water sampling (Supplementary Table 3). Nutrient concentrations (total dissolved inorganic nitrogen and phosphate) were <1 μM (Supplementary Table 3) and monthly satellite-derived chlorophyll *a* for Bremer Bay was, on average, higher in winter compared to summer for both years (i.e. 0.14 mg m^{-3} during 2014/15 summer to 0.79 mg m^{-3} during 2015 winter and 0.13 mg m^{-3} during 2015/16 summer to 0.46 mg m^{-3} during 2016 winter mg m^{-3}; Fig. 1d).

Photo-physiology

On average, F_v/F_m seasonally ranged from 0.45 to 0.65 (Fig. 2a). The lowest F_v/F_m (i.e. average of 0.45) occurred during the unusually cold El Niño winter period (Fig. 2a). Average seasonal F_v/F_m was significantly negatively correlated with light (r^2 = 0.37, Root Mean Squared Error (RMSE) = 0.050 F_v/F_m, p = 0.027; Supplementary Fig. S4), and there was a significant nonlinear (polynomial) relationship between average seasonal F_v/F_m and temperature (r^2 = 0.56, p = 0.012; Supplementary Fig. S4).

Coral calcification rates and extension rates

Mean rates of calcification over the entire study ranged from 0.16 to 0.45 mg cm^{-2} d^{-1}, and were thus almost three-fold higher during the winter months compared to the summer months (Fig. 2b). Calcification rates showed no significant relationship with temperature (r^2= 0.004, RMSE = 0.113 mg cm^{-2} d^{-2}, p = 0.857; Fig. 3a), but were significantly negatively correlated with light (r^2= 0.71, Root Mean Squared Error (RMSE) = 0.061 mg cm^{-2} d^{-2}, p < 0.001; Fig. 3b). The low F_v/F_m during the unusually cold El Niño winter period did not coincide with significantly lower calcification rates (i.e. compared to the October 2015 time point; $t(34)$ = 1.797, p = 0.081). Average linear extension rates ranged from 0.47 to 1.28 mm mo^{-1}, with higher extension rates during winter compared to summer (Supplementary Table 1).

Coral calcifying fluid chemical composition

Both Sr/Ca (Site 1: $r^2 = 0.62$, Site 2: $r^2 = 0.71$) and Li/Mg (Site 1: $r^2 = 0.67$, Site 2: $r^2 = 0.62$) were significantly correlated with ambient seawater temperature ($p<0.001$; Supplementary Fig. S5a-b), supporting that our sampling scheme captured different seasons of growth. On average, the $\delta^{11}B$ compositions varied seasonally by 2‰ ($\delta^{11}B$ ~23 to 25‰; Supplementary Fig. S6a), corresponding to seasonal ranges in pH_{cf} of 8.50 (summer) to 8.65 (winter) (Fig. 2c). Seasonal changes in pH_{cf} and temperature were inversely correlated ($r^2 = 0.46$, $p = 0.007$; Supplementary Fig. S7a), and changes in pH_{cf} were significantly positively linearly correlated with calcification rates ($r^2= 0.45$, RMSE = 0.086 mg cm^{-2} d^{-2}, $p = 0.017$; Fig. 3c). Skeletal ratios of boron to calcium (B/Ca) ranged from 0.57 to 0.73 mmol mol^{-1} (Supplementary Fig. S6b), which corresponded to mean $[CO_3^{2-}]_{cf}$ from ~780 to 930 µmol kg^{-1}, with higher $[CO_3^{2-}]_{cf}$ during winter compared to summer (Fig. 2d). Furthermore, $[CO_3^{2-}]_{cf}$ showed a significant positive relationship with calcification rates ($r^2= 0.68$; RMSE = 0.069 mg cm^{-2} d^{-2}, $p = 0.001$; Fig. 3d). DIC_{cf} was substantially elevated relative to ambient seawater by a factor of 1.5 to 2 (Fig. 2e), with lower DIC_{cf} during the first winter period, and anomalously high DIC_{cf} during the second winter period (i.e. during the 2016 El Niño winter) (Fig. 2e). Thus, there was no significant linear correlation between DIC_{cf} /DIC_{sw} and temperature ($r^2 = 0.10$, RMSE = 0.134, $p = 0.301$; Supplementary Fig. S7b), or between DIC_{cf} /DIC_{sw} and calcification rates ($r^2 = 0.002$, RMSE = 0.112 mg cm^{-2} d^{-2}, $p = 0.886$). There was, however, a significant negative correlation between DIC_{cf} /DIC_{sw} and pH_{cf} ($r^2 = 0.50$, RMSE = 0.022, $p = 0.009$; Supplementary Fig. S7c).

On average, $[Ca^{2+}]_{cf}$ ranged from 8.3 to 9.7 mmol kg^{-1}, and were thus 10 to 30% lower than seawater values (~10.7 to 11 mmol kg^{-1}; Fig. 2f). $[Ca^{2+}]_{cf}/[Ca^{2+}]_{sw}$ was negatively correlated with calcification rates ($r^2= 0.64$; RMSE = 0.072 mg cm^{-2} d^{-2}, $p = 0.002$; Fig. 3e), but showed no significant correlation with pH_{cf} ($r^2= 0.32$, RMSE = 0.215, $p = 0.63$; Supplementary Fig. S7d). Lastly, mean Ω_{cf} was relatively stable year-round ranging from just 10.3 to 11.2 (Fig. 2g); and thus, there was no significant linear relationship between Ω_{cf} and calcification rates ($r^2 = 0.005$, RMSE = 0.112 mg cm^{-2} d^{-2}, $p = 0.823$; Fig. 3f).

Discussion

(a) Drivers of the seasonal patterns of coral calcification

We found that the high-latitude coral *T. reniformis* exhibited unusual seasonal patterns of calcification, with three-fold higher calcification rates during winter compared to summer. This is in strong contrast to the well-established pattern of enhanced summer

289 calcification in both tropical [38,39] and high-latitude corals [8–11], providing novel insights
290 into the drivers and mechanisms supporting coral growth at its latitudinal limits. Our findings
291 are unexpected given that seasonally higher temperatures should have promoted faster growth
292 during summer compared to winter due to the strong temperature-dependence of aragonite
293 precipitation rates [22] and light-enhanced calcification [40]. For example, in tropical corals,
294 calcification rates typically increase with temperature until an optimum is reached, which is
295 usually equal to, or slightly above, the annual average temperatures experienced by the coral
296 (Fig. 3a) [38,39,41]. Moreover, along latitudinal temperature gradients, coral calcification
297 rates generally decline with increasing latitude (decreasing temperatures) and are much lower
298 than their tropical counterparts [42,43]. In contrast, our findings demonstrate that the positive
299 relationship between temperature and calcification rate observed in tropical corals is not
300 applicable to all high-latitude coral species.
301 Few other studies report area-normalised field-based calcification for *T. reniformis*.
302 Our rates of calcification during the winter (34.5°S; 0.3 to 0.5 mg cm^{-2} d^{-1}), however, were
303 within the range of other tropical and sub-tropical corals, such as *Pocillopora damicornis* at
304 both Rottnest Island (32°S; 0.3 to 0.9 mg cm^{-2} d^{-1}) [31] and Coral Bay, Ningaloo (21.5°S; 0.4
305 to 0.9 mg cm^{-2} d^{-1}) [14], despite the much cooler temperatures (i.e. 16 to 21°C at Bremer Bay
306 vs. 18 to 24°C at Rottnest and 22 to 28°C in Coral Bay, Ningaloo). This implies that corals in
307 Bremer Bay have altered their thermal tolerance range, via either adaptation or
308 acclimatisation, to support rates of calcification similar to tropical corals but at cooler
309 temperatures and lower light levels [44]. Thus, our findings based on corals in Bremer Bay
310 suggest that warming seawater temperatures may not necessarily accelerate coral
311 calcification at high-latitude, or be required to sustain calcification during winter. Our results
312 also provide additional support to a growing number of studies that have documented unusual
313 seasonal or latitudinal variability in coral calcification rates, and/or instances where coral
314 calcification rates were not maximised under the warmest conditions (i.e. summer and at low-
315 latitude) (i.e. [8,14,31,45,46]).
316 However, the mechanisms underlying faster growth during winter and at high-
317 latitude, are not yet fully understood; particularly for corals growing near their latitudinal
318 limits [23], and our study is among the first to provide insights into the mechanisms enabling
319 these patterns. One possible explanation for the lower growth rates during summer compared
320 to winter is that the corals may have experienced heat stress during the warmer summer
321 months resulting in suppressed summer growth rates [14,28]. However, this hypothesis is not

supported by measurements of F_v/F_m, which showed no signs of chronic photo-inhibition during the summer months (Fig. 2a). Furthermore, no visible signs of bleaching (i.e. paling of corals due to loss of photosynthetic pigments and/or symbionts) were observed throughout the study (authors observations). Nevertheless, F_v/F_m was negatively correlated with seasonal changes in light ($r^2 = 0.37$; Supplementary Fig. S4), such that these corals showed a seasonal photo-acclimatory response, with higher photosynthetic efficiency during winter under low light levels; similar to results from previous work, albeit in tropical locations [47].

(b) Mechanisms of coral calcification at their latitudinal limits

A more plausible explanation for the unusually high calcification rates in winter compared to summer is that the corals were able to dictate seasonal rates of calcification by modulating their internal chemistry to counter-act changes in the external conditions (i.e. temperature and light) [23]. For example, the absence of any temperature and light dependent seasonality in the calcification rates can be largely explained by higher winter-time pH_{cf} and $[CO_3^{2-}]_{cf}$ to support higher calcification rates during winter, despite the seasonally lower light, temperature, and DIC_{cf}. Meanwhile, during summer, reduced pH_{cf} and $[CO_3^{2-}]_{cf}$ corresponded to lower rates of calcification (Figs. 1, 4). Therefore, the unexpected negative relationship between seasonal light and calcification rates may have indirectly resulted from the concurrently higher up-regulation of pH_{cf} (and thus higher $[CO_3^{2-}]$) during winter (i.e. low light) compared to summer (i.e. high light).

Furthermore, we found that pH_{cf} was negatively correlated with DIC_{cf}, consistent with previous studies for tropical and sub-tropical corals (~0.1 to 0.2 pH units) [18,23]. Given that the process of pH up-regulation is thought to be relatively energetically inexpensive [15], healthy corals are able to systematically counter-regulate DIC_{cf} and pH_{cf} to maintain elevated Ω_{cf} [16,18,23]; therefore potentially regulating their calcification rates [15,23]. These seasonal changes in DIC_{cf} [18,23] were pro-cyclical with temperature and light (except during the 2016 El Niño winter), and thus consistent with temperature- and/or light-driven seasonal changes in metabolic CO_2 [21,48]. Furthermore, our results support a recent study showing that corals growing in a sub-tropical environment at Rottnest Island (located ~550 km north-west of Bremer Bay in WA) can maintain stable calcification rates year-round by modulating their calcifying fluid carbonate chemistry, such that the effect of seasonally varying temperature and light on rates of bulk calcification was dampened (see [23]).

Interestingly, the counter-regulation of DIC_{cf} and pH_{cf} appears to systematically shift biogeographically. Although we cannot rule out species specific differences, *T. reniformis*

shows higher pH_{cf} (~8.5 to 8.65 at 16 to 21°C) than both the sub-tropical corals at Rottnest Island (~8.4 to 8.6 at 18 to 24°C) and the tropical corals at Coral Bay (~8.3 to 8.55 at 22 to 28°C) and Lizard Island (~8.25 to 8.5 at 23 to 28.5°C) [18,23], consistent with a temperature-dependence of pH_{cf} regulation [18,23]. This trend occurs in the absence of any differences in absolute pH_{sw} values and independently of the magnitude of seasonal changes in pH_{sw} (i.e., ~8.03 to 8.10 at all locations). Thus, this physiological control on pH up-regulation appears to be a ubiquitous strategy among both high-latitude and tropical corals for counter-acting declines in metabolically-supplied DIC_{cf} [18,23].

However, other factors likely contribute to the capacity of *T. reniformis* to tolerate sub-optimal conditions (i.e. low light and temperature) and to calcify at faster rates during winter compared to summer. One possible explanation is that only the species that can heavily rely on heterotrophic feeding or have high environmental tolerance are able to survive in temperate reefs at high-latitude [12,49]. For example, in addition to the energy provided by their photosynthetic symbionts, corals can also meet their energy requirements by heterotrophic feeding on plankton, although this ability varies between species (e.g. see review [50]). Thus, another potential explanation for the unusual seasonality of calcification rates is a higher reliance on heterotrophy during winter when temperatures and light levels are low. The positive relationship between heterotrophic feeding and calcification rates is well-documented, particularly for temperate corals [12,51], and seasonal variability in feeding has been shown previously, for example, in the symbiotic temperate coral *Cladocora caespitosa* in the Mediterranean Sea, which switches between autotrophy during summer and heterotrophy during winter [52]. Chlorophyll *a* levels were higher in winter compared to summer in Bremer Bay (Fig. 1d), and a positive correlation between calcification rates and chlorophyll *a* has been demonstrated previously [43,11]. Assuming the higher wintertime chlorophyll *a* corresponded to increased heterotrophy, this may have contributed to higher calcification rates during winter compared to summer by maintaining metabolic energy required for key growth processes, such as pH_{cf} up-regulation, tissue growth and composition, and organic matrix synthesis (e.g. see review [50]).

The higher rate of skeletal $CaCO_3$ formation during winter resulted in a concurrent decline in $[Ca^{2+}]_{cf}$ (Fig. 3e). During summer, the opposite occurred whereby a reduction in calcification rate resulted in higher $[Ca^{2+}]_{cf}$ (albeit still 10% lower than the surrounding seawater), consistent with less Ca^{2+} being depleted during periods of lower calcification. The observed reduction in $[Ca^{2+}]_{cf}$ relative to seawater values (10 to 30% depending on rates of

calcification; Fig. 2b, Fig. 3e) is not surprising given that (i) $[Ca^{2+}]_{cf}$ should decline as it is depleted from the calcifying fluid during calcification (Fig. 4), and that (ii) $[Ca^{2+}]_{cf}$ is most likely not limiting calcification in *T. reniformis* because it is far greater (~8.3 to 9.8 mmol kg^{-1}) than $[CO_3^{2-}]_{cf}$ (~0.7 to 0.95 mmol kg^{-1}; Fig. 2). Thus, while elevating $[Ca^{2+}]_{cf}$ above seawater concentrations is important for driving calcification in some coral species (such as *Pocillopora damicornis* and *Galaxea fascicularis*) [26,29], this does not appear to be the case for *T. reniformis*.

Multiple mechanisms may operate to transport calcium and protons between seawater and the calcifying fluid. However, the active exchange of Ca^{2+} with H^+ using the enzyme Ca-ATPase at the site of calcification has long been considered the primary mechanism for corals to up-regulate both $[Ca^{2+}]_{cf}$ and pH_{cf} [17,53,54]. If Ca^{2+} up-regulation were operational in these corals due to the enzyme Ca-ATPase exchange of Ca^{2+} with H^+, we could expect simultaneously high $[Ca^{2+}]_{cf}$ and pH_{cf} caused by the pumping in of Ca^{2+} and the pumping out of H^+ to elevate pH_{cf} [29]. Yet, the opposite is observed here, such that $[Ca^{2+}]_{cf}$ was lowest when both pH_{cf} and calcification rates were highest (Fig. 2). $[Ca^{2+}]_{cf}$ may be initially elevated, but is then clearly outweighed by precipitation, given that $[Ca^{2+}]_{cf}/[Ca^{2+}]_{sw}$ is less than 1. Furthermore, if seasonally higher rates of calcification were causing a systematic decline in pH_{cf} due to an increase in protons when HCO_3^- is converted to CO_3^{2-} (i.e. instead of counter-balancing DIC_{cf}), then the lowest pH_{cf} would have occurred when calcification rates were highest. Conversely, we show here that seasonally higher rates of calcification did not cause a systematic decline in pH_{cf}, as would be expected if pH_{cf} and $[Ca^{2+}]_{cf}$ were controlled by the same processes (i.e. Ca-ATPase and $CaCO_3$ precipitation). Thus, while the up-regulation of $[Ca^{2+}]_{cf}$ may still be occurring [26], the reduction in $[Ca^{2+}]_{cf}$ when pH up-regulation is highest nevertheless suggests that mechanisms other than the ATP-ase driven exchange of H+ for Ca^{2+} must be involved in the supply of Ca^{2+} and up-regulation of pH_{cf} (e.g. Ca-channels, Ca^{2+}/Na^+ exchange, HCO_3^- pumps; Fig. 4) [21,53].

The seasonal dynamics of pH_{cf}, $[CO_3^{2-}]_{cf}$, $[Ca^{2+}]_{cf,}$ and calcification act to maintain relatively stable and elevated Ω_{cf} (10.7 ± 0.5) year-round (Fig. 2). However, the winter-time Ω_{cf}, for example, was far lower than it would be if constant levels of $[Ca^{2+}]_{cf}$ were maintained (e.g. at seawater concentrations) or if $[Ca^{2+}]_{cf,}$ were up-regulated above seawater values as it was for OA-resistant *P. damicornis* corals in a laboratory study [26]. Thus, Ω_{cf} is modulated by calcification through the depletion of $[Ca^{2+}]_{cf}$, such that decoupling between Ω_{cf} and rates of calcification can occur. This would explain why the observed seasonally fluctuating

growth rates do not mirror the relatively stable levels of Ω_{cf} (Fig. 2). If this is true, it implies that bulk coral calcification rates may not depend strongly on the instantaneous rate of aragonite crystal growth (i.e. Ω_{cf}), but rather on the supply of carbon to the site of calcification. Further, our results are consistent with recent work, albeit in tropical corals under both heat and acidification stress, which suggests an optimum threshold of Ω_{cf} is required for calcification to occur [16,28], but Ω_{cf} may not be the primary driver of calcification rates beyond this threshold. Thus, our results provide additional support to the hypothesis that maintaining a stable, yet elevated Ω_{cf}, is likely a prerequisite for biomineralization.

To explain how the modulation of the calcifying fluid carbonate chemistry resulted in the observed calcification rates, we have integrated our findings with the literature [18,21,53] to form a conceptual model that includes our measurements of both aspects of Ω_{cf} (i.e. CO_3^{2-} and Ca^{2+}) for corals growing at high-latitude (Fig. 4a-b). Firstly, pH up-regulation (removal of H^+) raises the availability of CO_3^{2-} at the site of calcification and elevates Ω_{cf}, thus promoting calcification (Fig. 4b) [15]. This is driven by (i) the diffusion of metabolic CO_2 into the calcifying fluid [21], and (ii) a shift in the equilibrium of DIC in favour of CO_3^{2-} over bicarbonate (HCO_3^-) (Fig. 4b). CO_2 is converted into bicarbonate using carbonic anhydrase (CA), producing additional H^+, and HCO_3^- may be brought to the site of calcification using bicarbonate transporters (BAT) [55]. Elevating pH works in conjunction with the supply of DIC to increase the availability of CO_3^{2-} (Fig. 4b). Lastly, calcification occurs and Ca^{2+} is depleted from the calcifying fluid, thereby causing a decrease in Ω_{cf} (Fig. 4b). Thus, the same Ω_{cf} can be achieved by either high CO_3^{2-} up-regulation and high calcification (i.e. more $[Ca^{2+}]_{cf}$ depleted), or low CO_3^{2-} up-regulation and low calcification (i.e. less $[Ca^{2+}]_{cf}$ depleted; Fig. 4b).

(c) Drivers and mechanisms of calcification during the 2016 El Niño winter cooling

The anomalous cold temperatures during the 2016 El Niño winter provide further insight into the extreme cold periods that are likely to threaten high-latitude corals more frequently than tropical corals [56]. *T. reniformis* showed significant cold stress (F_v/F_m: 0.47 ± 0.01) when temperatures dropped 1°C cooler (~16°C) than the normal winter minimum (~17°C). However, *T. reniformis* calcification rates did not appear to be affected by the El Niño-driven cold stress (Fig. 2), given that lower F_v/F_m did not correspond to significantly lower calcification rates (i.e. compared to the 2015 winter). The high calcification rates during this period of El Niño-driven cold stress were supported via unusually high up-

regulation of winter-time DIC_{cf}. This could potentially be explained by an increase in metabolic DIC supply via increased heterotrophy during sub-optimal or stressful conditions [57].

Our results show, however, that the higher levels of DIC_{cf} during the El Niño cold period were still counter-regulated systematically by lower pH_{cf} during winter in order to maintain stable Ω_{cf} and elevated $[CO_3^{2-}]_{cf}$ to support high rates of calcification (Fig. 3). Thus, Ω_{cf} during the 2016 winter was lower than it would be if the mechanism of pH_{cf} and DIC_{cf} counter-regulation were not operational. These results have important implications for high-latitude coral calcification during periods of ENSO-driven cold stress [56], as they demonstrate that corals are able to biologically modulate the carbonate chemistry of the calcifying fluid, with a shift to higher DIC_{cf}, to maintain calcification rates.

(d) High-latitude coral calcification mechanisms and the future of high-latitude corals

Under future climate change, rising temperatures at high-latitude could potentially have a positive effect on calcification rates, particularly during winter when growth rates are thought to be limited by lower temperatures [10]. We show here, however, that seasonally lower wintertime temperatures and light levels did not limit the calcification rates of *T. reniformis* corals at their latitudinal limits. Furthermore, these corals were able to maintain high rates of calcification despite an ENSO-driven cold stress event. The absence of any clear relationship between temperature and coral calcification rate can be explained by (i) higher chlorophyll *a* during winter compared to summer providing the coral nutrition for increased heterotrophy, and (ii) the corals' ability to modulate pH_{cf} in response to seasonally variable DIC_{cf}, such that seasonal changes in bulk rates of calcification appear to depend strongly on $[CO_3^{2-}]_{cf}$, rather than Ω_{cf} or temperature. Thus, warmer seawater temperatures due to continued ocean warming may not necessarily promote faster rates of calcification at high-latitude, and are not necessarily required to support high-latitude coral calcification during winter [31]. Moreover, marine heatwaves have recently caused mass bleaching of high-latitude reefs [5]. Thus, further work is required to establish how high-latitude coral calcification rates will respond to the combined effects of OA, warming, and marine heatwaves.

References

1. Reaka-Kudla ML. 1997 The Global Biodiversity of Coral Reefs: A comparison with Rain Forests. *Biodivers. II Underst. Prot. Our Biol. Resour.*, 83–108. (doi:10.2307/1791071)
2. Veron J. 1995 *Corals in space and time: the biogeography and evolution of the Scleractinia.* London, pp 1-321: Cornell Univ. Press, Ithaca.
3. Hoegh-Guldberg O *et al.* 2007 Coral reefs under rapid climate change and ocean acidification. *Science (80-.).* **318**, 1737–1742. (doi:10.1126/science.1152509)
4. Hughes TP *et al.* 2017 Global warming and recurrent mass bleaching of corals. *Nature* (doi:10.1038/nature21707)
5. Le Nohaïc M, Ross CL, Cornwall CE, Comeau S, Lowe R, McCulloch MT, Schoepf V. 2017 Marine heatwave causes unprecedented regional mass bleaching of thermally resistant corals in northwestern Australia. *Sci. Rep.* **7**, 14999. (doi:10.1038/s41598-017-14794-y)
6. Marubini F, Ferrier-Pages C, Cuif J-P. 2003 Suppression of skeletal growth in scleractinian corals by decreasing ambient carbonate-ion concentration: a cross-family comparison. *Proc. Biol. Sci.* **270**, 179–84. (doi:10.1098/rspb.2002.2212)
7. Comeau S, Edmunds PJ, Spindel NB, Carpenter RC. 2014 Fast coral reef calcifiers are more sensitive to ocean acidification in short-term laboratory incubations. *Limnol. Oceanogr.* **59**, 1081–1091. (doi:10.4319/lo.2014.59.3.1081)
8. Sawall Y, Al-Sofyani A, Hohn S, Banguera-Hinestroza E, Voolstra CR, Wahl M. 2015 Extensive phenotypic plasticity of a Red Sea coral over a strong latitudinal temperature gradient suggests limited acclimatization potential to warming. *Sci. Rep.* **5**, 8940. (doi:10.1038/srep08940)
9. Kuffner IB, Hickey TD, Morrison JM. 2013 Calcification rates of the massive coral

Siderastrea siderea and crustose coralline algae along the Florida Keys (USA) outer-reef tract. *Coral Reefs* **32**, 987–997. (doi:10.1007/s00338-013-1047-8)

10. Crossland C. 1984 Seasonal variations in the rates of calcification and productivity in the coral *Acropora formosa* on a high-latitude reef. *Mar Ecol Prog Ser* **15**, 135–140. (doi:10.3354/meps015135)
11. Courtney TA *et al.* 2017 Environmental controls on modern scleractinian coral and reef-scale calcification. *Sci. Adv.* **3**, e1701356. (doi:10.1126/sciadv.1701356)
12. Miller MW. 1995 Growth of a temperate coral: effects of temperature, light, depth, and heterotrophy. *Mar Ecol Prog Ser* **122**, 217–225.
13. Edmunds PJ. 2011 Zooplanktivory ameliorates the effects of ocean acidification on the reef coral *Porites* spp. *Limnol. Oceanogr.* **56**, 2402–2410. (doi:10.4319/lo.2011.56.6.2402)
14. Foster T, Short J., Falter JL, Ross C, McCulloch MT. 2014 Reduced calcification in Western Australian corals during anomalously high summer water temperatures. *J Exp Mar Biol Ecol* **461**, 133–143.
15. McCulloch MT, Falter JL, Trotter J, Montagna P. 2012 Coral resilience to ocean acidification and global warming through pH up-regulation. *Nat. Clim. Chang.* **2**, 1–5. (doi:10.1038/nclimate1473)
16. Schoepf V, Jury CP, Toonen R, McCulloch M. 2017 Coral calcification mechanisms facilitate adaptive response to ocean acidification. *Proc. R. Soc. B* (doi:10.1098/rspb.2017.2117)
17. Venn A, Tambutté É, Holcomb M, Allemand D, Tambutté S. 2011 Live tissue imaging shows reef corals elevate pH under their calcifying tissue relative to seawater. *PLoS One* **6**, e20013. (doi:10.1371/journal.pone.0020013)
18. McCulloch MT, D'Olivo Cordero JP, Falter J, Holcomb M, Trotter JA. 2017 Coral

537 calcification in a changing World: the interactive dynamics of pH and DIC up-
538 regulation. *Nat. Commun.* , 1–8. (doi:10.1038/ncomms15686)
539 19. Wall M, Ragazzola F, Foster LC, Form a., Schmidt DN. 2015 Enhanced pH up-
540 regulation enables the cold-water coral *Lophelia pertusa* to sustain growth in aragonite
541 undersaturated conditions. *Biogeosciences Discuss.* **12**, 6757–6781. (doi:10.5194/bgd-
542 12-6757-2015)
543 20. Georgiou L, Falter JL, Trotter J, Kline DI, Holcomb M, Dove SG, Hoegh-Guldberg O,
544 McCulloch MT. 2015 pH homeostasis during coral calcification in a free ocean CO_2
545 enrichment (FOCE) experiment, Heron Island reef flat, Great Barrier Reef. *Proc. Natl.*
546 *Acad. Sci.* , 201505586. (doi:10.1073/pnas.1505586112)
547 21. Cohen AL, McConnaughey TA. 2003 Geochemical Perspectives on Coral
548 Mineralization. *Rev. Mineral. Geochemistry* **54**, 151–187. (doi:10.2113/0540151)
549 22. Burton EA, Walter LM. 1987 Relative precipitation rates of aragonite and Mg calcite
550 from seawater: Temperature or carbonate ion control? *Geology* **15**, 111.
551 (doi:10.1130/0091-7613(1987)15<111:RPROAA>2.0.CO;2)
552 23. Ross CL, Falter JL, McCulloch MT. 2017 Active modulation of the calcifying fluid
553 carbonate chemistry (δ^{11}B, B/Ca) and seasonally invariant coral calcification at sub-
554 tropical limits. *Sci. Rep.* **7: 13830**, 1–11. (doi:10.1038/s41598-017-14066-9)
555 24. Holcomb M, Venn AA, Tambutté E, Tambutté S, Allemand D, Trotter J, McCulloch
556 M. 2014 Coral calcifying fluid pH dictates response to ocean acidification. *Sci. Rep.* **4**,
557 5207. (doi:10.1038/srep05207)
558 25. DeCarlo TM, D'Olivo JP, Foster T, Holcomb M, Becker T, McCulloch MT. 2017
559 Coral calcifying fluid aragonite saturation states derived from Raman spectroscopy.
560 *Biogeosciences Discuss.* , 1–25. (doi:10.5194/bg-2017-194)
561 26. DeCarlo TM, Comeau S, Cornwall CE, Mcculloch MT. 2018 Coral resistance to ocean

562 acidification linked to increased calcium at the site of calcification. (In Press) *Proc. R.*
563 *Soc. B Biol. Sci.*
564 27. Wall M, Fietzke J, Schmidt GM, Fink A, Hofmann LC, Beer D De, Fabricius KE.
565 2016 Internal pH regulation facilitates in situ long-term acclimation of massive corals
566 to end-of-century carbon dioxide conditions. *Sci. Rep.* , 1–7. (doi:10.1038/srep30688)
567 28. D'Olivo JP, McCulloch MT. 2017 Response of coral calcification and calcifying fluid
568 composition to thermally induced bleaching stress. *Sci. Rep.*, 1–15.
569 (doi:10.1038/s41598-017-02306-x)
570 29. Al-Horani F, Al-Moghrabi, de Beer D. 2003 The mechanism of calcification and its
571 relation to photosynthesis and respiration in the scleractinian coral *Galaxea*
572 *fascicularis*. *Mar Biol* **142**, 419–426. (doi:10.1007/s00227-002-0981-8)
573 30. Veron JEN, Marsh LM. 1988 Hermatypic corals of Western Australia: records and
574 annotated species list. *Rec West Aust Mus*, 1–136.
575 31. Ross CL, Falter JL, Schoepf V, McCulloch MT. 2015 Perennial growth of hermatypic
576 corals at Rottnest Island, Western Australia (32°S). *PeerJ* **3**, e781.
577 (doi:10.7717/peerj.781)
578 32. IMOS. 2018 IMOS Ocean Colour (2015 and 2016).
579 *http://oceancurrent.imos.org.au/oceancolour.php (accessed 2018-04-11)*.
580 33. Bak R. 1973 Coral weight increment in situ. A new method to determine coral growth.
581 *Mar Biol* **20**, 45–49. (doi:10.1007/BF00387673)
582 34. Trotter J *et al.* 2011 Quantifying the pH 'vital effect' in the temperate zooxanthellate
583 coral *Cladocora caespitosa*: Validation of the boron seawater pH proxy. *Earth Planet.*
584 *Sci. Lett.* **303**, 163–173. (doi:10.1016/j.epsl.2011.01.030)
585 35. Dickson AG. 1990 Thermodynamics of the dissociation of boric acid in synthetic
586 seawater from 273.15 to 318.15 K. *Deep Sea Res. Part A. Oceanogr. Res. Pap.* **37**,

587 755–766. (doi:10.1016/0198-0149(90)90004-F)
588 36. Klochko K, Kaufman AJ, Yao W, Byrne RH, Tossell J a. 2006 Experimental
589 measurement of boron isotope fractionation in seawater. *Earth Planet. Sci. Lett.* **248**,
590 261–270. (doi:10.1016/j.epsl.2006.05.034)
591 37. Holcomb M, DeCarlo TM, Gaetani GA, McCulloch MT. 2016 Factors affecting B/Ca
592 ratios in synthetic aragonite. *Chem. Geol.* **437**, 67–76.
593 (doi:10.1016/j.chemgeo.2016.05.007)
594 38. Marshall AT, Clode P. 2004 Calcification rate and the effect of temperature in a
595 zooxanthellate and an azooxanthellate scleractinian reef coral. *Coral Reefs* **23**, 218–
596 224. (doi:10.1007/s00338-004-0369-y)
597 39. Vajed Samiei J, Saleh A, Mehdinia A, Shirvani A, Kayal M. 2015 Photosynthetic
598 response of Persian Gulf acroporid corals to summer versus winter temperature
599 deviations. *PeerJ* **3**, e1062. (doi:10.7717/peerj.1062)
600 40. Gattuso J-P, Allemand D, Frankignoulle M. 1999 Photosynthesis and calcification at
601 cellular, organismal and community levels in coral reefs: a review on Interactions and
602 control by carbonate chemistry. *Amer Zool* **39**, 160–183.
603 41. Jokiel PL, Coles SL. 1977 Effects of Temperature on the Mortality and Growth of
604 Hawaiian Reef Corals*. *Mar Biol* **208**, 201–208.
605 42. Carricart-Ganivet JP. 2004 Sea surface temperature and the growth of the West
606 Atlantic reef-building coral *Montastraea annularis*. *J. Exp. Mar. Bio. Ecol.* **302**, 249–
607 260. (doi:10.1016/j.jembe.2003.10.015)
608 43. Lough JM, Cantin NE, Benthuysen JA, Cooper TF. 2016 Environmental drivers of
609 growth in massive *Porites* corals over 16 degrees of latitude along Australia's
610 northwest shelf. *Limnol. Oceanogr.* **61**, 684–700. (doi:10.1002/lno.10244)
611 44. Clausen CD, Roth AA. 1975 Effect of temperature and temperature adaption on

612 calcification rate in the hermatypic coral *Pocillopora damicornis*. *Mar Biol* **33**, 93–
613 100.
614 45. Roik A, Roder C, Röthig T, Voolstra CR. 2015 Spatial and seasonal reef calcification
615 in corals and calcareous crusts in the central Red Sea. *Coral Reefs* **35**.
616 (doi:10.1007/s00338-015-1383-y)
617 46. Goffredo S, Caroselli E, Mattioli G, Pignotti E, Dubinsky Z, Zaccanti F. 2009 Inferred
618 level of calcification decreases along an increasing temperature gradient in a
619 Mediterranean endemic coral. *Limnol. Oceanogr.* **54**, 930–937.
620 (doi:10.4319/lo.2009.54.3.0930)
621 47. Warner ME, Chilcoat GC, McFarland FK, Fitt WK. 2002 Seasonal fluctuations in the
622 photosynthetic capacity of photosystem II in symbiotic dinoflagellates in the
623 Caribbean reef-building coral *Montastraea*. *Mar. Biol.* **141**, 31–38.
624 (doi:10.1007/s00227-002-0807-8)
625 48. Furla P, Galgani I, Durand I, Allemand D. 2000 Sources and mechanisms of inorganic
626 carbon transport for coral calcification and photosynthesis. *J Exp Biol* **203**, 3445–57.
627 49. Mizerek TL, Baird AH, Beaumont LJ, Madin JS. 2016 Environmental tolerance
628 governs the presence of reef corals at latitudes beyond reef growth. *Glob. Ecol.*
629 *Biogeogr.* (doi:10.1111/geb.12459)
630 50. Houlbrèque F, Ferrier-Pagès C. 2009 Heterotrophy in tropical scleractinian corals. *Biol*
631 *Rev Camb Philos* **84**, 1–17.
632 51. Rodolfo-Metalpa R, Peirano a., Houlbrèque F, Abbate M, Ferrier-Pagès C. 2008
633 Effects of temperature, light and heterotrophy on the growth rate and budding of the
634 temperate coral *Cladocora caespitosa*. *Coral Reefs* **27**, 17–25. (doi:10.1007/s00338-
635 007-0283-1)
636 52. Ferrier-Pages C, Peirano A, Abbate M, Cocito S, Negri A, Rottier C, Riera P, Rodolfo-

637 Metalpa R, Reynaud S. 2011 Summer autotrophy and winter heterotrophy in the
638 temperate symbiotic coral *Cladocora caespitosa*. *Limnol. Oceanogr.* **56**, 1429–1438.
639 53. Allemand D, Ferrier-Pagès C, Furla P, Houlbrèque F, Puverel S, Reynaud S, Tambutté
640 É, Tambutté S, Zoccola D. 2004 Biomineralisation in reef-building corals: from
641 molecular mechanisms to environmental control. *Comptes Rendus Palevol* **3**, 453–467.
642 (doi:10.1016/j.crpv.2004.07.011)
643 54. McConnaughey TA. 1994 Ion transport and the generation of biomineral
644 supersaturation. In *7th International Symposium Biomineralization* (eds D Allemand,
645 J-P Cuif), pp. 1–18. Monaco.
646 55. Zoccola D *et al.* 2015 Bicarbonate transporters in corals point towards a key step in the
647 evolution of cnidarian calcification. *Sci. Rep.* **5**, 9983. (doi:10.1038/srep09983)
648 56. Saxby T, Dennison WC, Hoegh-Guldberg O. 2003 Photosynthetic responses of the
649 coral *Montipora digitata* to cold temperature stress. *Mar. Ecol. Prog. Ser.* **248**, 85–97.
650 (doi:10.3354/meps248085)
651 57. Ezzat L, Towle E, Irisson J-O, Langdon C, Ferrier-Pagès C. 2015 The relationship
652 between heterotrophic feeding and inorganic nutrient availability in the scleractinian
653 coral *T . reniformis* under a short-term temperature increase. *Limnol. Oceanogr.* , n/a-
654 n/a. (doi:10.1002/lno.10200)
655

656 ## Acknowledgments

657 Thanks to A. Comeau, K. Rankenburg, and J. Pablo D'Olivo for assistance in the
658 coral isotope and mass spectrometry laboratories. We are grateful to Craig and Anne Lebens
659 at Bremer Bay Dive and all volunteers (H. Clarke, C. Bowyer, A. Kuret, M. Cuttler, S. Bell,
660 E. Lester, Y. Mulders, G. Ellwood, and C. Krause) for assistance in the field. The authors
661 acknowledge the facilities, and the scientific and technical assistance of the Australian
662 Microscopy & Microanalysis Research Facility at the Centre for Microscopy,

Characterisation & Analysis, The University of Western Australia, a facility funded by the University, State and Commonwealth Governments.

Funding

This research was supported by funding provided by an ARC Laureate Fellowship (LF120100049) awarded to Professor M. McCulloch, the ARC Centre of Excellence for Coral Reef Studies (CE140100020), and an Australian Post Graduate Scholarship awarded to C. Ross.

Author contributions

C.R. designed the experiments, conducted all fieldwork and laboratory work, analysed the data, and wrote the manuscript. V.S contributed to experimental design, participated in fieldwork, and guided data analysis. T.D. conducted laboratory work, and guided data analysis. M.M. contributed to experimental design, participated in fieldwork. All authors contributed to manuscript drafts.

Competing interests

There are no competing financial interests.

Availability of data

Data will be available at the Zenodo Digital Repository (10.5281/zenodo.1220102).

Ethics statement

The activities for this study were conducted under permission from the Government of Western Australia Department of Parks and Wildlife (DPaW) with research permits and license to take fauna for scientific purposes (#SF010109 and #SF010963) and the Government of Western Australia Department of Fisheries with research permits and exemption from the Fish Resources Management Act 1994 (#2944 and #2410). All local regulations and permit requirements were followed. This study did not require clearance by the UWA Animal Ethics Committee.

Figure Legends

Figure 1. (a) Location of the study sites. (**b**) Daily averaged seawater temperature (°C), (**c**) weekly averaged photosynthetically active radiation (PAR) reaching the benthos, and (**d**) monthly satellite-derived chlorophyll *a* for Bremer Bay (obtained from IMOS, [32]). Shading denotes winter and no shading denotes summer. Seasons are defined based on changes in light and temperature.

Figure 2. Time series of (**a**) photochemical efficiency (F_v/F_m) (**b**) calcification rates, (**c**) pH, (**d**) DIC, (**e**) $[CO_3^{2-}]$, (**f**) $[Ca^{2+}]$, and (**g**) Ω for *T. reniformis* in Bremer Bay. Values represent mean ± 1 s.d for calcifying fluid (cf) parameters (n = 5 per site) and mean ± 1 s.e for calcification rates and F_v/F_m (n = 14 at Site 1, n = 21 at site 2). No shading denotes summer, light shading denotes winter, and dark shading denotes El Niño winter cooling.

Figure 3. Sensitivity of coral calcification rate to (**a**) temperature (fitted with a conceptual non-linear polynomial temperature growth curve), (**b**) photosynthetically active radiation (calcification rate = -0.021 PAR + 0.677), (**c**) pH_{cf} (calcification rate = 1.27 pH_{cf} – 10.57), and (**d**) $[CO_3^{-2}]_{cf}$ (best fitted by the exponential relationship calcification rate = $0.0007e^{0.0069x}$). (**e**) Relationship between $[Ca^{2+}]_{cf}/[Ca^{2+}]_{sw}$ with calcification rates (best fitted by the polynomial relationship: $[Ca^{2+}]_{cf}/[Ca^{2+}]_{sw}$ = 1.4313 calcification rate^2 - 1.2104G + 1.0377), and (**f**) sensitivity of calcification rate to Ω_{cf}. Values represent the mean ± 1 SE (calcifying fluid: n = 5 per site; calcification: n = 14 at Site 1, n = 21 at site 2). Asterisks denote statistical significance.

Figure 4. Schematics of the (**a**) coral calcification mechanisms [18,21,53], and (**b**) calcification processes. Scleractinian corals create their calcium carbonate skeletons within an extracellular calcifying fluid located between the sub-calicoblastic cells and the skeleton with fluid supplied from the seawater [53]. Coral pH up-regulation occurs via the pumping of H^+ out of the calcifying fluid, promoting the diffusion of metabolic CO_2 from the mitochondria (M) into the calcifying fluid. CO_2 is converted into bicarbonate using carbonic anhydrase (CA) producing additional H^+, and active transport using bicarbonate transporters (BAT) also occurs [55]. Metabolic CO_2 is also supplied to the symbionts (Z) [48,55]. pH up-regulation shifts the equilibrium of DIC in favour of carbonate (CO_3^{2-}) relative to bicarbonate (HCO_3^-), producing additional H^+. Calcification occurs and Ca^{2+} is depleted from the calcifying fluid, causing a decrease in Ω_{cf}. Multiple mechanisms of calcium transport may operate (e.g. Ca-ATPase, Ca-channels, and Ca^{2+}/Na^+ exchange), combined with seawater renewal, to re-supply Ca^{2+} for calcification.

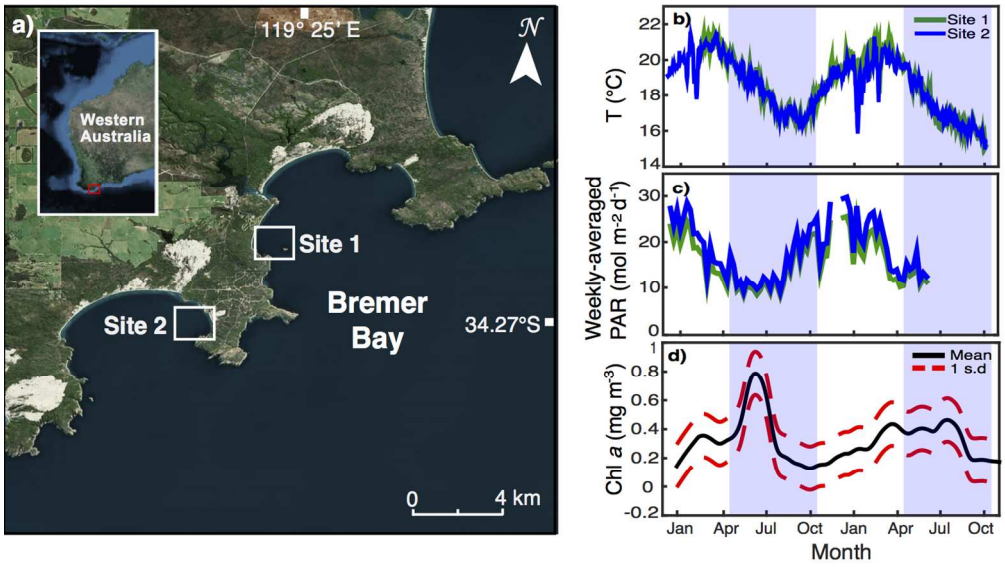

Figure 1. (**a**) Location of the study sites. (**b**) Daily averaged seawater temperature (°C), (**c**) weekly averaged photosynthetically active radiation (PAR) reaching the benthos, and (**d**) monthly satellite-derived chlorophyll a for Bremer Bay (obtained from IMOS, [32]). Shading denotes winter and no shading denotes summer. Seasons are defined based on changes in light and temperature.

134x75mm (300 x 300 DPI)

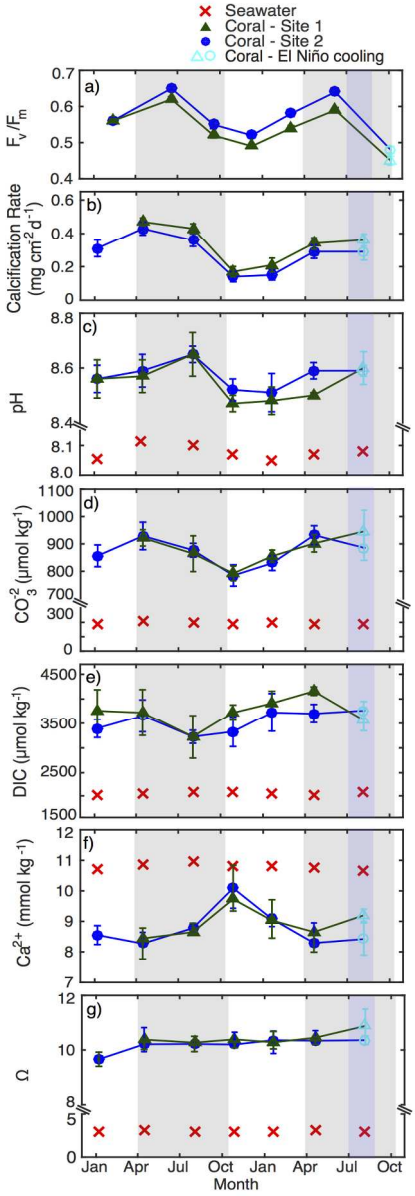

Figure 2. Time series of (**a**) photochemical efficiency (F_v/F_m) (**b**) calcification rates, (**c**) pH, (**d**) DIC, (**e**) [CO_3^{2-}], (**f**) [Ca^{2+}], and (**g**) Ω for *T. reniformis* in Bremer Bay. Values represent mean ± 1 s.d for calcifying fluid (cf) parameters (n = 5 per site) and mean ± 1 s.e for calcification rates and F_v/F_m (*n* = 14 at Site 1, *n* = 21 at site 2). No shading denotes summer, light shading denotes winter, and dark shading denotes El Niño winter cooling.

83x238mm (300 x 300 DPI)

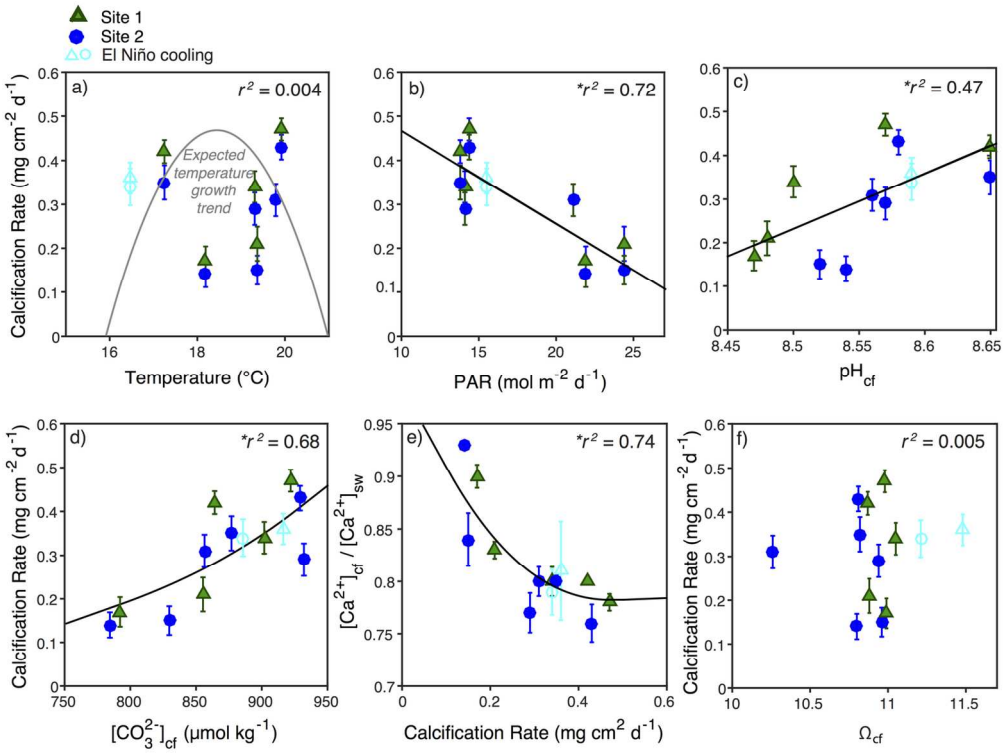

Figure 3. Sensitivity of coral calcification rate to (**a**) temperature (fitted with a conceptual non-linear polynomial temperature growth curve), (**b**) photosynthetically active radiation (calcification rate = -0.021 PAR + 0.677), (**c**) pH_{cf} (calcification rate = 1.27 pH_{cf} – 10.57), and (**d**) $[CO_3^{2-}]_{cf}$ (best fitted by the exponential relationship calcification rate = 0.0007e0.0069x). (**e**) Relationship between $[Ca^{2+}]_{cf}/[Ca^{2+}]_{sw}$ with calcification rates (best fitted by the polynomial relationship: $[Ca^{2+}]_{cf}/[Ca^{2+}]_{sw}$ = 1.4313 calcification rate 2 - 1.2104 calcification rate + 1.0377), and (**f**) sensitivity of calcification rate to Ω_{cf}. Values represent the mean ± 1 SE (calcifying fluid: *n* = 5 per site; calcification: *n* = 14 at Site 1, *n* = 21 at site 2). Asterisks denote statistical significance.

143x108mm (300 x 300 DPI)

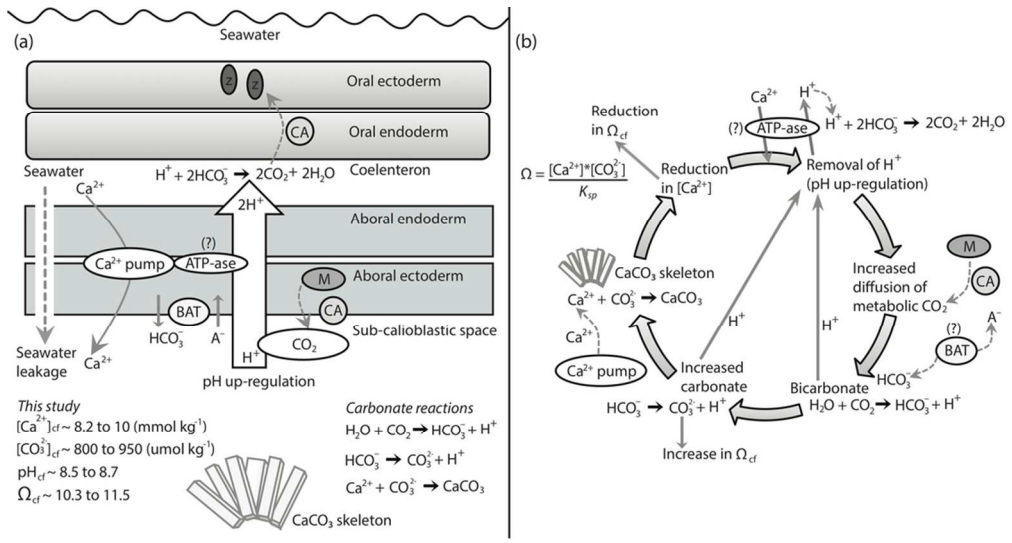

Figure 4. Schematics of the (**a**) coral calcification mechanisms [18,21,53], and (**b**) calcification processes. Scleractinian corals create their calcium carbonate skeletons within an extracellular calcifying fluid (cf) located between the sub-calioblastic cells and the skeleton with fluid supplied from the seawater [53]. Coral pH up-regulation occurs via the pumping of H^+ out of the calcifying fluid, promoting the diffusion of metabolic CO_2 from the mitochondria (M) into the calcifying fluid. CO_2 is converted into bicarbonate using carbonic anhydrase (CA) producing additional H^+, and active transport using bicarbonate transporters (BAT) also occurs [55]. Metabolic CO_2 is also supplied to the symbionts (Z) [48,55]. pH up-regulation shifts the equilibrium of DIC in favour of carbonate (CO_3^{2-}) relative to bicarbonate (HCO_3^-), producing additional H^+. Calcification occurs and Ca^{2+} is depleted from the calcifying fluid, causing a decrease in Ω_{cf}. Multiple mechanisms of calcium transport may operate (e.g. Ca-ATPase, Ca-channels, and Ca^{2+}/Na^+ exchange), combined with seawater renewal, to re-supply Ca^{2+} for calcification.

95x50mm (300 x 300 DPI)